

Description of neutron β -decay in gas phase in terms of developed polaronic exciton concept

Alexander V. Udal'tsov*

Lomonosov Moscow State University, Vorobjovy Gory 1, 119234 Moscow, Russia.

ABSTRACT

Weak interactions transforming protons to neutrons or vice versa were considered in terms of developed polaronic exciton concept and chemical physics. The suggested model describes events of neutron β -decay and the spectrum and explains why free neutron is the most long-lived among the other meta-stable particles. Gas-phase water as the environment for the β -decay reaction mimicking that in Earth atmosphere implies that neutron β -decay occurs under mediation of hydrogen-bonded water molecules since neutron hydration is impossible to avoid because water forms clusters even at high vacuum. Proton sharing frequency of 3.45238 ± 0.01016 THz found earlier in the hydrogen-bonded molecules of water clusters generates the charge oscillations. The oscillation or microwave photon absorption produces energy gap between $2S_{1/2}$ and $2P_{1/2}$ electron levels in the hydrated neutron generating a meta-stable state. An estimate of the energy gap and the consideration of neutron β -decay events allowed to calculate neutron lifetime that is found to be 882.118 s. The latter is in a good agreement with averaged neutron lifetime of 881.5 ± 1.5 s. The energy gap estimation allowed to conclude that the spectrum of cosmic microwave background radiation corresponding to that of blackbody radiation originates under neutron creation from strongly coupled opposite charges located on the oxygen atom of hydrogen-bonded water molecule. Distribution of kinetic energy of

the electrons glued with antineutrino emitted under neutron β -decay is found consistent with the measured β -decay spectrum.

KEYWORDS: neutron β -decay, neutron lifetime, β -decay spectrum, polaronic exciton, cosmic microwave background.

CONTENTS

1. Introduction
2. Theory
3. Results and discussion
 - 3.1. Polaronic exciton generation in hydrogen-bonded molecules of gas-phase water
 - 3.2. Consideration of neutron β -decay and the backward reaction in gas-phase water under polaronic exciton generation in hydrogen-bonded water molecules
 - 3.3. Evaluation of neutron lifetime at β -decay
 - 3.4. Simulation of the energy spectrum of electrons from neutron β -decay according to the suggested model
4. Conclusions
- Appendix A1
- Appendix A2
- Appendix A3
- Conflict of Interest Statement
- References

1. Introduction

Free neutron is the most long-lived among the meta-stable particles; it has a lifetime ca. 14-15 min, at the same time neutron β -decay and the simplest nuclear reactions play an important role in cosmology [1, 2]. Weak interactions, which are the subject of

*Corresponding author: Komintern Street, 9-2-29, Moscow 129327, Russia.
Email id: avu151@yandex.ru

nuclear physics, transform protons to neutrons and if the transformation occurs in gas-phase water, then the interactions are the subject of chemical physics too. Neutrino and antineutrino, the elementary particles with half-integer spin, which have no electric charge and pass through usual matter unimpeded and undetected, are usually involved in the reactions with participation of neutron. Experimental mean lifetime of neutron is 885.7 s [3], although the later average value is 881.5 s [4], while a measurement with a gravitational trap for ultra cold neutrons gave 878.5 s [5]. The reaction of neutron β -decay, which takes place in the Earth atmosphere [1], in fact occurs in gas-phase water environment that implies the presence of hydrated neutrons. Neutron hydration is impossible to avoid because its lifetime is long [2-4]. Thus, neutron lifetime and the β -decay reaction are of interest to many researchers because both have important implications in particle physics and cosmology.

According to the *Standard Model* of particle physics, neutron β -decay reaction occurs *via* the so-called virtual W^- boson, which possesses a high energy and therefore a large mass [2]. In electrodynamics particle mass is considered as the coefficient of proportionality between the velocity and the particle momentum that can be the sum of mechanic and electromagnetic momenta [6]. Theoretical evaluation of neutron lifetime gives 951 s [2] and that estimation did not consider the meta-stable state of virtual W^- boson. In contrast to the virtual particle, a natural boson is generated in super-cooled water [7, 8] or in amorphous glass materials with hydrogen-bonded molecules [9, 10]. Behavior of such boson is described in terms of polaronic exciton concept [11, 12] and spin correlation effect [13] that is valid for the opposite charges too and plays a key role. Therefore, hydrogen bonding between molecules in gas phase containing the hydrated neutrons, which is a cause of charge oscillations, affects the processes involving neutron participation. This paper reports further results in the development of polaronic exciton theory applied for an estimate of microwave radiation energy, evaluation of neutron lifetime through consideration of meta-stable state, and behavior of real boson generated between hydrogen-bonded molecules that will reveal the important role of water in the Universe evolution.

2. Theory

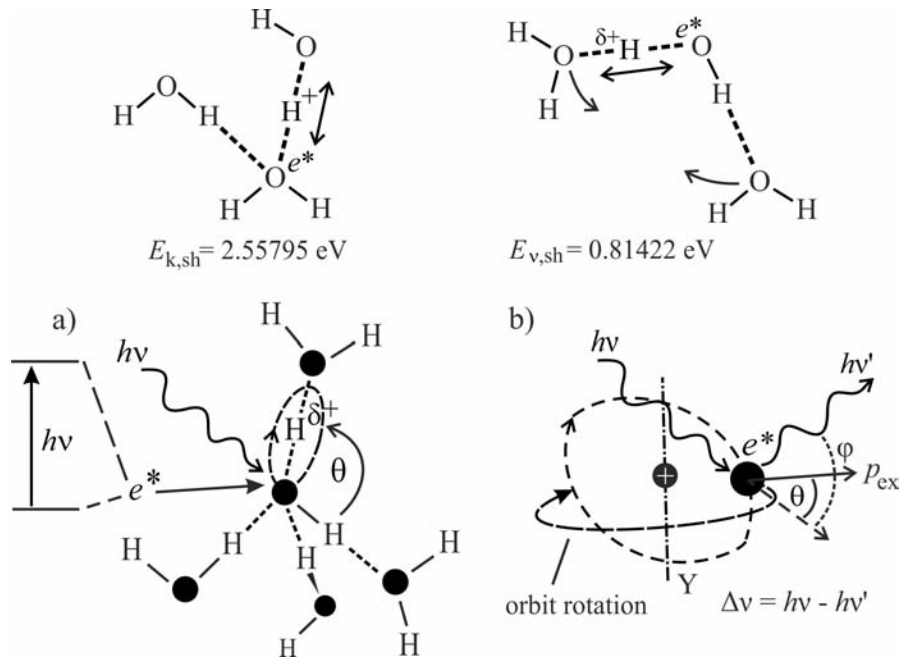
Polaronic exciton-coupled model was suggested for the description of vacuum ultraviolet spectrum of gas-phase water under incident photon interaction with water resulting in polaronic exciton generation [14], where the absorption spectrum in the energy range 8.5-10 eV is interpreted in terms of polaronic exciton rotation coupled with proton sharing. In the excited state polaronic exciton has kinetic energy that equals excitation energy when a photon is absorbed. Therefore, polaronic exciton kinetic energy can be defined *via* momentum $p_{ex} = \hbar k$ as depicted in Scheme 1b depending on the interaction θ angle [14]. Then polaronic exciton radii, which are defined as the average distance between hole and electron, are proved dependent on the interaction angle and therefore angular momentum quantum number is defined by number of electrons in the external electronic shell. Thus, polaronic exciton kinetic energy (E_k) can be written *via* the momentum of polaronic exciton [15].

$$E_k = p_{ex}^2 / (2M_{ef}) \quad (1)$$

or

$$E_k = 2\hbar^2 (2\pi/r_{ex})^2 / M_{ef} \quad (1a),$$

where M_{ef} is polaronic exciton effective mass, $M_{ef} = m_{ef}^h + m_{ef}^e$ ($M_{ef} = 10.5m_e$), $p_{ex} = 2\pi(\hbar/\lambda)$ or $p_{ex} = \hbar k$, $k = 2\pi/r_{ex}$, where k is the wavenumber. The masses of hole (m_{ef}^h) and electronic polarons (m_{ef}^e) in condensed matter are $m_{ef}^h = 10m_e$ and $m_{ef}^e = 0.5m_e$ (or $m_{ef}^h = 9.51m_e$ for more accurate calculation) [16, 17], $m_e = 9.1093819 \times 10^{-31}$ kg. As known, relation similar with Eq. (1) is given for exciton in quantum well that is called the confinement energy, which is increased by the amount $\Delta E = \hbar^2 k^2 / (2M_{ef})$ relative to the unconfined state. However, in the case of polaronic exciton, the strong coupling between the opposite charges allows to consider the wavenumber as a combination of four harmonic oscillators resulting in harmonic mean of polaronic exciton radius (r_{ex}) [15]. Therefore, kinetic energy depending on the r_{ex} value according to Eq. (1a) (or excitation energy), which includes energies of polaronic exciton generation and proton sharing ($E_{k,sh}$ or $E_{v,sh}$), defines which proton is shared when an electron absorbs a photon [11] as displayed in Scheme 1, inset. Thus, two possible modes of proton sharing can happen in water depending on the excitation energy.



Scheme 1. Illustration of the incident photon interaction with water: a) resulting in polaronic exciton generation under a photon absorption that leads to vibrational mode of proton sharing with $E_{v,sh} = 0.81422 \text{ eV}$; and b) producing electron coupling with proton that is accompanied by the electron orbit rotation after the photon absorption (with momentum p_{ex} and θ angle) or the photon scattering on the electron, where ϕ and $h\nu'$ are the scattering angle and the outgoing photon, respectively. Inset shows two modes of proton sharing in the local structures, which require different energies $E_{k,sh}$ and $E_{v,sh}$.

When proton of the excited molecule is borrowed for proton sharing, the energy ($E_{v,sh}$) required for this (vibrational) mode calculated at elastic approximation with the coefficient $k_e = m_{ef}^e \omega_a^2$ is 0.81422 eV [15]. But when proton of the neighboring hydrogen-bonded H_2O molecule is borrowed for proton sharing as depicted in Scheme 1, inset (to the left), the required energy ($E_{k,sh}$) is 2.55795 eV for the kinetic mode of proton sharing [18], $E_{k,sh}/E_{v,sh} = \pi$ exactly [15, 18]. Polaronic exciton can be stabilized in the ground state that is defined by the bound state energy ($E_{ex,b}$), for gas-phase water $E_{ex,b} = -2.052 \text{ eV}$ [14, 18]. Physical model used for the description of inelastic interaction under the photon absorption as displayed in Scheme 1b is similar to the model of *Compton* scattering on electron. The similarity of the models allows to describe the interactions through θ angle, the angle between the incident photon direction and the electron momentum (see Scheme 1b) that is considered in details in Ref. [14]. Thus, the coefficient (β) that is proportional to *Compton wavelength* assumes the meaning of the spin-orbit coupling;

so $\sqrt{\beta}$ for electron and proton both forming the quasiparticle gives $(\sqrt{\beta})^2$, $\beta = 1.19100654$ [14, 19].

In the case of the incident x-ray photon interaction with water, the spin-orbit coupling parameter $\beta = 1.19100654$ involves six $2p$ -electrons of the oxygen atom and only one external electron of the hydrogen-bonded molecule; therefore this parameter is almost independent of the quaternary molecule coordination. Angular momentum of the electron operating like electronic polaron with the mass m_{ef}^e is $m_{ef}^e v r = \hbar[l(l+1)]^{1/2}$ that can be rewritten as follows taking into account a proportionality [19].

$$2\pi m_{ef}^e \omega r_{ex}^2 = \hbar [l(l+1)]^{1/2} \quad (2),$$

where ω is the angular frequency and l is the angular momentum quantum number, l is an integer in the range $7 \geq l \geq -7$. The form of Eq. (2) is constrained by the proportionality between $[l(l+1)]^{1/2}/2\pi = 1.19100654$ obtained with the quantum number $l = 7$ and spin-orbit coupling $\beta = 1.19100654$ defined as $\beta = 1/[2\pi(\cos \theta_m - \cos \theta_{m-1})]$, where $\Delta \cos \theta_m = \cos \theta_m - \cos \theta_{m-1} = 0.13363062$ (see details elsewhere [12, 19]). The angular frequency (ω) for electron

operating like electronic polaron is given by Eq. (3) [19].

$$\omega = \omega_{a,el} + \Delta\omega = \omega_{a,el} + [2\Delta E_k / (m_{ef}^e r_{ex}^2)]^{1/2} \quad (3),$$

where ΔE_k is the difference of kinetic energy calculated with the decrease of r_{ex} by $\lambda_C/2\pi$ step [18, 19] and $\omega_{a,el}$ is the angular frequency obtained under elastic interaction with the incident photon, $\omega_{a,el} = 1.13105 \times 10^{16} \text{ s}^{-1}$ [15]. Eqs. (2) and (3) represent the system, the solving of which allows to estimate both r_{ex} and ω [19] (see Appendix A1). A peculiarity of the frequency behavior is that the angular frequency of the electron unrestrictedly increases with the decrease of the polaronic exciton radius and this is a prerequisite for deuteron [19] and therefore for neutron creation.

We should consider important characteristics such as s - p -splitting between $2S_{1/2}$ and $2P_{1/2}$ electron levels in polaronic exciton again because it has direct relation to microwave radiation called cosmic microwave background [20, 21]. Earlier a diagram [19] for the illustration of levels of electron coupled with hole polaron as compared to the energy levels of hydrogen in the ground state was depicted according to *Feynman's* explanation of 21 cm wavelength [22]. However, spin-spin interaction under strong coupling between the opposite charges exhibits similar behavior as that of nuclear forces. That is to say, the opposite charges with antiparallel spins tend to avoid one another at a short distance that is compared with *Bohr radius*. While at resonance conditions under strong coupling in the hydrogen-bonded molecules, energy levels of the opposite charges are governed by golden section ($R_{gold} = \{1 + \sqrt{5}\}/2$) according to experimental results [11]. Then, we can connect the energy gap that arises in hydrogen atom in the ground state and the s - p -splitting between $2S_{1/2}$ and $2P_{1/2}$ electron levels in hydrogen atom known as *Lamb shift* [23]. The simplest explanation of *Lamb shift* consists in that the effect originates because the electron and proton with antiparallel spins tend to avoid one another like two electrons with the parallel spins [12]. Therefore, similar nature of the spin-spin interactions allows to connect both in a relation, namely the frequencies for the ground state $f_H = 1420405751.8 \pm 0.028 \text{ Hz}$ [22] and for the hydrogen in the excited state (*Lamb shift*) $f_L = 1057.864 \text{ MHz}$ [23]. On one hand, the opposite charges with antiparallel spins in the

ground state should tend to avoid one another increasing the energy gap proportionally to the golden section that governs energy levels under the strong coupling. While in the excited state, the distance between the opposite charges is larger; therefore, the repulsive spin correlation effect should be diminished. Hence, taking into account spin-orbit coupling parameter ($\sqrt{\beta}$) for the coupling of proton and the electron in the excited state to each other ($\sqrt{\beta}$)², we can write the following relations, where the spin-orbit coupling (β) for the ground state with the frequency (f_{gH}) should be excluded with the factor β^{-1} .

$$f_{gH} = R_{gold} f_L / \beta \quad (4),$$

or

$$f_L = \beta f_{gH} / R_{gold} \quad (4a)$$

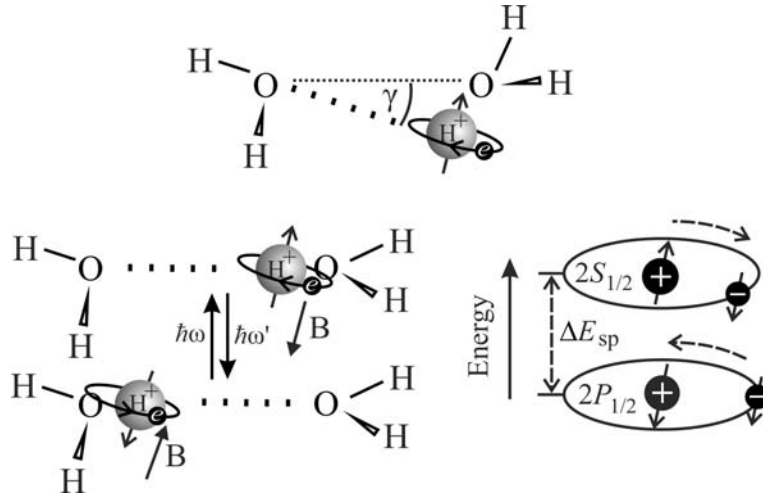
With $\beta = 1.19100654$ and experimental $f_H = 1420405751.8$ the calculated $f_L = 1045.53585 \text{ MHz}$. The latter is an agreement with theoretical frequency of 1052.1 MHz obtained by Bethe, Kroll & Lamb, French & Weisskopf [24]; the deviation from 1052.1 MHz is 0.6%. The ratio (R_{gold}/β) means the repulsive effect between the antiparallel spins of the opposite charges in hydrogen ground state relative to that when its electron is in the excited state.

Thus, the energy gap (ΔE_{sp}) between $2S_{1/2}$ and $2P_{1/2}$ -electron levels under proton moving in the hydrogen-bonded water molecules as depicted in Scheme 2 accompanied by proton spin turnover, which is estimated using Eqs. (4) and (5), is somewhat changed in comparison with the previous value of 1.41149 cm^{-1} theoretically derived earlier [12, 25]. Under hydrogen bonding, which leads to an increase of the confined energy, the energy gap is proportional to the energy gap of the generated polaronic exciton (ΔE_{pln}) with the coefficient R_{gold} under three-dimension walk of the electron ($\beta^{3/2}$) coupled with the proton [12].

$$\Delta E_{sp} = R_{gold} \Delta E_{pln} = \Delta E_L (\sqrt{\beta})^3 R_{gold} (m_{ef}^h / m_{ef}^e) \quad (5)$$

With $f_L = 1045.53585 \text{ MHz}$ (energy gap $\Delta E_L = 0.03487532 \text{ cm}^{-1}$) the calculated $\Delta E_{pln} = 0.8621840 \text{ cm}^{-1}$ and $\Delta E_{sp} = 1.395043 \text{ cm}^{-1}$.

Thus, s - p -splitting between $2S_{1/2}$ and $2P_{1/2}$ electron levels of polaronic exciton in hydrogen-bonded molecules (ΔE_{sp}) under the excitation originates like in hydrogen atom. Therefore, an energy gap (ΔE_{mwr})



Scheme 2. Illustration of proton moving accompanied by the nucleus spin turnover exhibiting boson behavior [12] that results in the energy gap ΔE_{sp} between $2S_{1/2}$ and $2P_{1/2}$ -electron levels (on the right) ($\hbar\omega - \hbar\omega')/2\pi = \Delta E_{sp}$ and short-living polaronic exciton (in the upper water dimer). Inset shows a bend of H-bond under libration of hydrogen-bonded molecules with proton/hydrogen deflection on γ angle from the straight hydrogen bond that diminishes the orbit overlapping under the spin-orbit coupling.

in the quasiparticle composed by hole polaron strongly coupled with the electron with antiparallel spins in the ground state should be proportional to the s - p -splitting in an excited state (ΔE_{sp}) with the same coefficient (R_{gold}/β). The ground state of the quasiparticle emits a microwave photon when the energy gap ΔE_{mwr} disappears under neutron creation (see below). Thus, the following relation defines this energy gap.

$$\Delta E_{mwr} = (R_{gold}/\beta)\Delta E_{sp} \quad (6)$$

With $\Delta E_{sp} = 1.395043 \text{ cm}^{-1}$ the calculated $\Delta E_{mwr} = 1.8952263 \text{ cm}^{-1}$ that corresponds to the temperature 2.726805 K . The spectrum of the microwave radiation with a maximum at 158.6 GHz calculated using *Planck law* has been reproduced with the obtained $T=2.726805 \text{ K}$ (see Appendix A2). The spectrum is found in good agreement with *COBE FIRAS Data* [26]. Thus, the spectrum of cosmic microwave background radiation corresponding to that of the blackbody radiation originates from strongly coupled electron and proton located on the oxygen atom of hydrogen-bonded water molecule under neutron creation. Nowadays the temperature of cosmic microwave background (CMB) is 2.725 - 2.726 K , which is well consistent with the result of *COBE FIRAS* [21]; therefore the obtained $T=2.726805 \text{ K}$ is in good agreement with the latter.

In the hydrogen-bonded water molecules proton can operate like boson [12], which absorbs in the infrared region of spectra [7-8, 27-28]. Description of the real boson behavior allows to estimate proton-sharing frequency in tetrahedron, i.e. tetrahedral hydrogen bonding oscillations that is $3.45238 \pm 0.01016 \text{ THz}$ averaged with earlier obtained values of 3.448024 , 3.4574081 , 3.4582796 , and 3.4458 THz [12, 29]. The model suggested below implies that only antineutrino, which has the positive spin projection on its momentum (positive helicity), can glue the coupled electron and proton with parallel spins in polaronic exciton or hydrated neutron, since in this case antineutrino has the positive spin projection on the electron momentum too.

3. Results and discussion

3.1. Polaronic exciton generation in hydrogen-bonded molecules of gas-phase water

Fig. 1 shows x-ray absorption spectrum of gas-phase water published earlier [30] with energy levels evaluated with the use of polaronic exciton concept discussed in Ref. [18]. In gas-phase water, an electron absorbing x-ray photon should accumulate kinetic energy like in the case of liquid water [18]. The energy accumulated by the electron in liquid water is 14.005934 eV [19], which is calculated through the energy ($E_{k,sh}$) of kinetic mode of proton

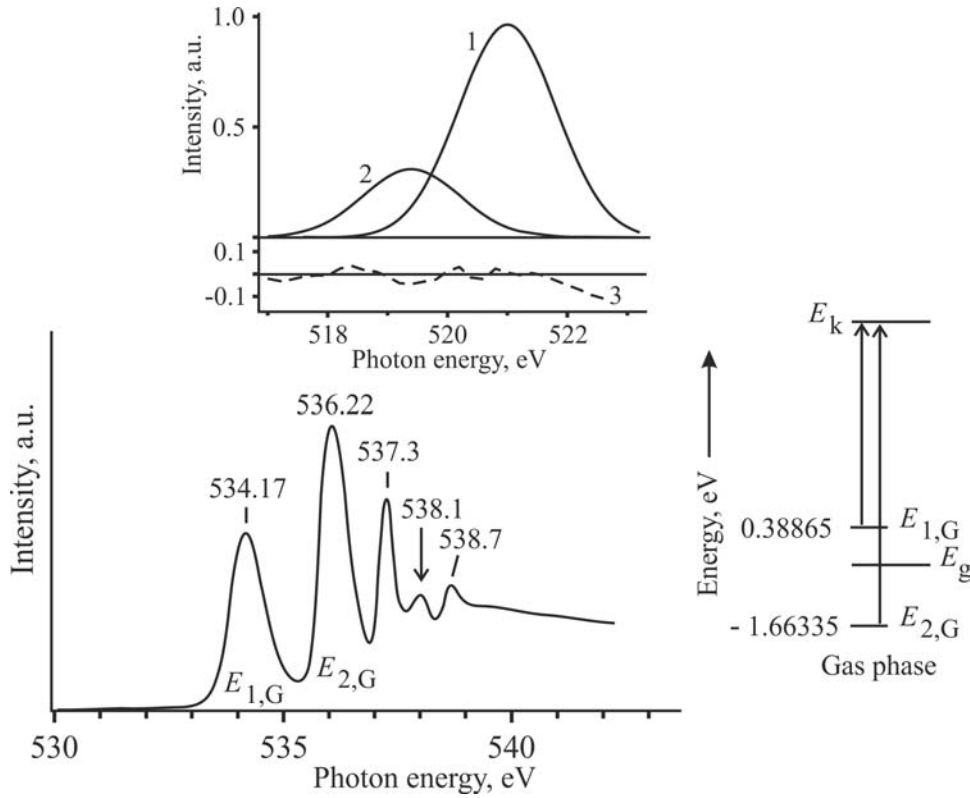


Fig. 1. X-ray absorption spectrum of gas-phase water reproduced using data from Ref. [18], where a band of $E_{1,G}$ is located at 534.17 eV due to the electronic bonding $E_{e-Hb} = 0.425566$ eV. Insets show (to the right): diagram of energy levels for gas-phase water, where E_g and E_k are the ground state level and kinetic energy, respectively, evaluated using Eq. (1) that is $E_{k,g} = 534.556$ eV without inelastic effect [18, 19]. Upper: simulation of x-ray emission spectrum of water molecules fitted using two *Gauss* functions with $\sigma = 0.81422$ eV and a maximum around: (1) 521.0 eV; (2) ca. 519.4 eV; and (3) the difference between their sum and data calculated using experimental spectrum reported in Ref. [32]; the pressure in the experimental chamber was 1×10^{-9} Torr.

sharing, spin-orbit coupling (β_q) depending on quaternary molecule coordination that is $\beta_q = \pi\beta$ [11, 12], and Rydberg constant (R_∞). In gas phase the difference between kinetic energy $E_{k,g} = 534.556$ eV and main emission at 521.0 eV as displayed in Fig. 1, inset, curve 1 attests the accumulation of the less energy which is 13.556 eV. But with inelastic effect of libration ($E_{k,g} + 395 \text{ cm}^{-1}/8065.544 = 534.60497$ eV, $\nu_{L1} = 395.5 \text{ cm}^{-1}$ [31]), the same difference of 13.60497 eV is close to Rydberg constant ($R_\infty = 13.60569172$ eV). Similar calculation for the emission around 519.4 eV (Fig. 1, inset, curve 2) gives 14.02225 eV ($534.60497 - E_{v,sh} - \hbar\omega - 519.4 = 14.02225$ eV) taking into account proton sharing energy ($E_{v,sh}$) and longitudinal optical (LO) phonons with the energy $\hbar\omega$, i.e. inelastic effects decreasing the kinetic energy. The energy of LO phonons generated by hole polaron moving

along hydrogen bonds is $\hbar\omega = 0.3685$ eV [19]. In this case the value of 14.02225 eV is in agreement with the above 14.005934 eV. Thus, the emission of the second component at ca. 519.4 eV implies the presence of at least water dimers in gas phase because of proton sharing, but not single molecules under a high vacuum of 1×10^{-9} Torr [32] (1 Torr = 1/760 atm). However, in fact this emission implies the presence of water tetrahedrons in which LO phonons can move along hydrogen bonds [16].

Thus, both components of the emission spectrum attest the energy accumulation by the electron of the same water molecule being in the excited state or by the other electron of the neighboring hydrogen-bonded H_2O , which is coupled with the same proton. In the latter case, the accumulated kinetic energy is the same as that in liquid water with the deviation of 0.1%. The energy accumulated by electron can

be retained for some time in the ground state of hydronium ion after x-ray photon emission because of the stabilization of polaronic exciton in the bound state due to proton sharing between hydrogen-bonded molecules. Hence, the formed activated state with polaronic exciton confined in tetrahedron can serve as a molecular reactor like in the case of deuterium creation in the liquid under x-ray absorption [18].

Relaxation time (τ_r) for the generated polaronic exciton stabilized in the bound state as hydronium ion (H_3O^+) within the tetrahedron can be estimated with Eyring equation.

$$\tau_r = k_{tr} (h/k_B T) \exp(-E_{ac}/RT), \quad (7)$$

or

$$\tau_r = k_{tr} (h/k_B T) \exp(-\varepsilon_{ac}/k_B T) \quad (7a)$$

where ε_{ac} is the activation energy, h and k_B are *Planck* and *Boltzmann* constants, respectively and k_{tr} is the transmission coefficient. After x-ray photon emission, the generated polaronic exciton falls in the bound state on the next level $E_{2,G}$ with proton sharing, energy of which is 0.81422 eV [18]. Therefore, the activation energy (ε_{ac}) corresponds to the barrier of 0.84913 eV (see Fig. 1, inset, to the right) that is the sum $-1.66335 + 0.81422 = -0.84913$ eV. In Eq. (7a) the coefficient $k_{tr} = 1$ because de-coupling of the paired spins of the polaronic exciton occurs if the energy required for the activation is absorbed producing irreversible decay of the polaronic exciton bound state. Thus, with $\varepsilon_{ac} = -0.84913$ eV (6848.695 cm^{-1}) and $k_B T = 203.6454 \text{ cm}^{-1}$ ($T = 293 \text{ K}$) the calculated $\tau_r = 66.045$ s. In contrast, the relaxation time of the bound state in Earth atmosphere at -10°C ($T = 263 \text{ K}$) is expected to be 56.837 min.

3.2. Consideration of neutron β -decay and the backward reaction in gas-phase water under polaronic exciton generation in hydrogen-bonded water molecules

Free neutron β -decay into proton and electron is described according to the *Standard Model* of particle physics as follows, where $\bar{\nu}_e$ is electronic antineutrino [2].



According to well-known *Feynman* diagram, neutron transforms into proton and a virtual W^- boson that

itself decays into the electron and $\bar{\nu}_e$. There is an alternative instead of virtual W^- boson, because an actual boson can be generated in the excited state of hydrogen-bonded water molecules [11, 12]. This natural boson originates from a water molecule under proton sharing because of tetrahedral hydrogen bonding oscillations [12]. Nucleons and electrons are spin 1/2 fermions, which means their intrinsic angular momentum projected on an arbitrary direction can take on only the values of $\pm(1/2)\hbar$. In the hydrogen-bonded molecules, proton moving confined between oxygen atoms as displayed in Scheme 2 should be accompanied by the nucleus spin turnover induced by THz frequency absorption with $\hbar\omega$ energy that produces a short-living polaronic exciton state [25]. The hydrogen-bonding relaxation requires one more spin turnover in the course of the process of proton moving in the backward direction that is accompanied by $\hbar\omega'$ emission (see Scheme 2); hence the angular momentum projected on the z-axis gives the integer spin. This process of proton moving defines the second (or fast) Debye relaxation time (τ_2), which is 0.17902 ps calculated using the averaged frequency ($f_{\text{tHb}} = 3.45238 \text{ THz}$, see above) of tetrahedral hydrogen bonding oscillations ($\tau_2 = 1/(R_{\text{gold}} f_{\text{tHb}})$ [25]). The relaxation time 179.02 fs is consistent with the experimental value 182 fs measured by Mischa Bonn's group [12]. So the behavior of the confined proton is described to be like that of bosons [11, 12]. However, in the case of the hydrated neutron, the s - p -splitting between $2S_{1/2}$ and $2P_{1/2}$ electron levels inside the neutron, which is produced by a microwave photon absorption, should be retained until β -decay acts as described below in spite of the hydrogen bonding oscillations. Under strong interaction between the opposite charges, the confined proton exhibiting boson-like behavior can mediate weak interactions as evidenced below. Therefore, it can be called w -boson too.

It should be stressed that formalism of neutron β -decay implies that the emitted neutrino particle has positive helicity, that is antineutrino [2]. The w -boson moving within four-dimension quantum well of the hydrogen-bonded water molecules in tetrahedron implies that the formed meta-stable state should be the same as for the β -decay, reaction (A) as well as for the reaction (B). In the backward reaction of neutron creation antineutrino

collides with proton that eliminates the s - p -splitting between $2S_{1/2}$ and $2P_{1/2}$ electron levels.

$$p + e + \bar{\nu}_e \rightarrow n + \nu_{mwr} \quad (\text{B}),$$

where ν_{mwr} is a microwave radiation (mwr) photon that is emitted when an energy gap (ΔE_{sp}) [12], which arises because of repulsive spin-spin interaction between proton and electron composing the quasiparticle, i.e. s - p -splitting between $2S_{1/2}$ and $2P_{1/2}$ electron levels (see Appendix A3) disappears producing neutron. Note that antineutrino collision with proton is required for neutron creation; so the microwave photon is emitted in the ground state. Therefore, in fact the energy gap ΔE_{mwr} disappears generating the mwr -photon. The model suggested below for the description of weak interactions in the meta-stable state suggests that antineutrino glues the opposite charges in neutron.

In neutron β -decay reaction, mwr -photon absorption or charge oscillations because of hydrogen bonding in tetrahedron converts the hydrated neutron into the meta-stable state with the energy gap between the $2S_{1/2}$ and $2P_{1/2}$ electron levels. Therefore, the meta-stable state of the hydrated neutron, which exists due to hydrogen bonding oscillations in tetrahedron, defines the longer lifetime of the neutron as compared to the other meta-stable particles. The neutron lifetime is considered in the next section.

Under antineutrino collision with proton in the reaction (B), the energy of neutrino particle that is $E_\nu = p_\nu^2/(2m_\nu)$ is transformed into the proton momentum (p_p) and a residual momentum (p_{mwr}). The energy of the latter $E_{mwr} = E_\nu - p_p^2/(2m_p)$ should be emitted when the oscillating opposite charges disappear producing neutron. Therefore, according to the law of energy-momentum conservation, we can write the following relation with momenta before and after the collision, where k_{trW} is the coefficient of the coupling in the w -boson, or k_{trW}^{-1} is the transmission coefficient in the course of mwr -photon generation (ν_{mwr}).

$$p_\nu^2 = p_p (p_{mwr} k_{trW}^{-1}) \quad \text{or,}$$

$$(p_\nu/p_p) = k_{trW}^{-1} (p_{mwr}/p_\nu) \quad (8)$$

Without the contribution of p_{mwr} , which is negligible as compared with p_p , the transmission coefficient is defined as $k_{trW}^{-1} = 1/(\sqrt{\beta} + \sqrt{\beta}) = 0.458155528$.

Microwave radiation emitted by the oscillating charges in the meta-stable state under neutrino

creation should depend on spin-orbit coupling of the opposite charges. There are two electrons in the $\text{O}^{\ominus}\text{---H}^{\oplus}\text{---O}$ moiety coupled with the same proton in the tetrahedron; this means that two polaronic excitons with the energy gap ΔE_{pln} under strong coupling with proton sharing (or bipolaron) should have the increased energy gap as $\Delta E_{mwr} = 2\sqrt{\beta}\Delta E_{pln}$ since the proton is coupled with both electrons. According to *Pauli* principle, this state can exist only with antiparallel spins of the electrons, therefore until antineutrino collision or the state relaxation. In fact, the latter relation is the definition of above transmission coefficient expressed as follows.

$$k_{trW}^{-1} = (2\sqrt{\beta})^{-1} = \Delta E_{pln}/\Delta E_{mwr} \quad (9)$$

With $\Delta E_{pln} = 0.8723500855 \text{ cm}^{-1}$ (see Appendix A3) the calculated $\Delta E_{mwr} = 1.9040479 \text{ cm}^{-1}$ that corresponds to temperature $T = 2.739497 \text{ K}$, which is somewhat higher than $T_0 = 2.725\text{--}2.726 \text{ K}$ or 2.728 K of cosmic microwave background [21, 26].

In the reaction (B), after antineutrino collision with hydrated proton confined in tetrahedron that results in the proton spin turnover and microwave photon emission, the proton has the right-handed spin. In this case, the antineutrino interacting with the coupled proton and electron is glued with the latter because spin projection of the neutrino particle on its momentum (positive or right helicity) coincides with the electron moving direction as depicted in Fig. 2, inset b). In the relativistic case, the vertexes of the interacting neutrino particle and the electron should create a new vertex because of the different velocities of these particles, i.e. should create a gluon. This type of gluon is created in the course of the spin-spin interactions between antineutrino and the electron; therefore, instead of colored gluons partaking in hard interactions, it should be colorless because it is a ninth linear combination. According to quantum chromodynamics and the *Standard Model* of particle physics, the strong nuclear force, which binds quarks together inside the nucleons, is mediated by gluons that must carry a color-anticolor charge. So the particles carrying this force (called gluons) must occur in color anti-color units, i.e. the linear color-anticolor combination gives nine types of gluons. But the linear combination red anti-red + blue anti-blue + green anti-green (the ninth combination) must be non-interacting since the combination is colorless.

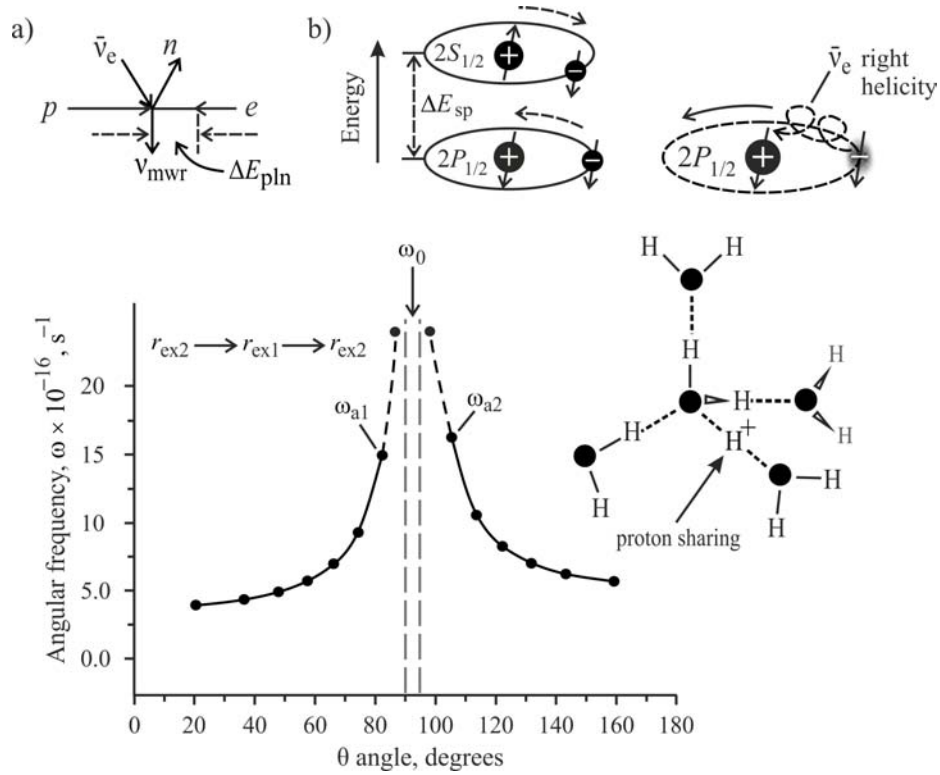


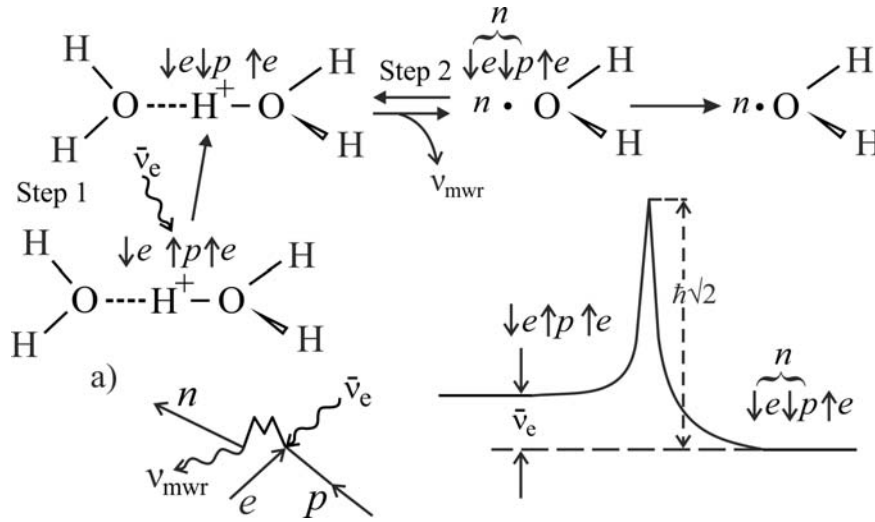
Fig. 2. Plot of angular frequency (see Appendix A1) for the electron coupled with the proton shared in the tetrahedron versus the interaction (θ) angle as displayed on the right. In Eq. (2), the expression $\hbar[l(l+1)]^{1/2}=0$ when $l=0$ or $l=-1$, therefore both values imply $r_{ex} \rightarrow 0$ while the corresponding angular frequency increases unrestrictedly (depicted by black dots out of the range). The direction $r_{ex} \rightarrow 0$ of the electron moving mediated by w -boson defines resonance angular frequency (ω_0) approximated by the pathway $r_{ex2} \rightarrow r_{ex1} \rightarrow r_{ex2}$. Insets show illustration of: a) neutron creation in the reaction (B); and b): spin correlation effect (to the left) and antineutrino interaction with the electron coupled with the proton in polaronic exciton when the interacted vertexes create a gluon (to the right).

Thus, there can only be eight gluons mediating the strong interactions. At the same time, the colorless gluon can exist only as the confined elementary particle that originates due to the interaction between the vertexes moving with different velocities.

This confined gluon, which glues neutrino particle with the electron, most likely cannot have an antiparticle because the nature of the vertex creating the gluon is independent of left or right helicity of neutrino particle, i.e. the vertex nature remains the same for both cases. As known neutrino particle participates only in weak interactions, while gluons participate in hard interactions accompanied by gravitation. Furthermore, the gluon does not carry a fixed energy, since they are massless particles [2, 4]. Thus, antineutrino properties provide the gluon creation when the electron occupies $2P_{1/2}$ -electron level as displayed in Fig. 2,

inset b) (to the right). Then with the decrease of polaronic exciton radius, when the angular frequency increases unrestrictedly as displayed in Fig. 2, the glued electron can acquire a velocity close to relativistic while the w -boson fluctuating state exists in the tetrahedron.

The energy initiating these reactions, antineutrino momentum or mwr -photon, defines the direction of the electron moving with $r_{ex} \rightarrow 0$ correlated with w -boson motion or in the backward direction. As mentioned above, the model implies that antineutrino glues the opposite charges in neutron. Therefore, the w -boson formation should involve the electron, proton and antineutrino simultaneously as depicted in Scheme 3a. Thus, antineutrino collision with the proton of the short-living polaronic exciton (depicted in Scheme 3 with the spins of $\downarrow e \uparrow p \uparrow e$) changes the nucleus spin direction to the opposite



Scheme 3. Illustration of the meta-stable state with $\hbar\sqrt{2}$ height barrier and the steps of neutron creation according to inset a) that illustrates the reaction between electron, proton and antineutrino producing neutron, where the overturned W is the actual w -boson, whose movement within the four-dimension quantum well outlined by tetrahedron structure mediates the weak interactions. The w -boson itself decays into neutron and microwave radiation photon.

that leads to the meta-stable state formation and w -boson fluctuations. As mentioned above, the collision of antineutrino with the proton eliminates the s - p -splitting between $2S_{1/2}$ and $2P_{1/2}$ electron levels that result in mwr -photon emission and neutron creation.

In addition, the suggested model explains why antineutrino passes through usual matter unimpeded and undetected. Proton moving between hydrogen-bonded molecules produces short-living polaronic exciton [25] that can create neutron if antineutrino collides with the proton. The collision produces the nucleus spin turnover and microwave photon emission. But if antineutrino collides with the proton in the lower structure of hydrogen-bonded molecules as depicted in Scheme 2, then this action results in short-living polaronic exciton state because of the nucleus spin turnover. However, the latter state is rapidly relaxed because it has very short lifetime [25].

3.3. Evaluation of neutron lifetime at β -decay reaction

Neutron β -decay is the reverse reaction of neutron creation considered above. As mentioned in Eq. (2), the expression $\hbar[l(l+1)]^{1/2}=0$ when $l=0$ or $l=-1$, both values imply unrestricted increase of the angular frequency as depicted by black dots in Fig. 2

out of the range. The latter is the prerequisite for the transformation of proton into neutron. Eq. (2) is valid for both reactions since the meta-stable state should be the same. Then for the reaction (B), the resonance angular frequency (ω_0) can be estimated for the extreme conditions that are $l=1$ ($r_{ex1} = 0.186666 \text{ \AA}$) and $l=-2$ ($r_{ex2}=0.178896 \text{ \AA}$) just before $r_{ex} \rightarrow 0$ leading to neutron creation. Therefore, the direction of the electron moving with 2π turn within the four-dimension quantum well outlined by tetrahedron structure defines the pathway $r_{ex2} \rightarrow r_{ex1} \rightarrow r_{ex2}$ and the frequency ω_0 (see Fig. 2). Thus, we arrive to $\omega_0 = 1.5941057 \times 10^{17} \text{ s}^{-1}$ with $r_{ex} = 0.180808 \text{ \AA}$ obtained at harmonic approximation according to the pathway. In the case of β -decay reaction, the electron in the meta-stable state moves in the direction with the increase of r_{ex} . So the pathway $r_{ex1} \rightarrow r_{ex2} \rightarrow r_{ex1}$ defines the resonance angular frequency $\omega_0 = 1.5276903 \times 10^{17} \text{ s}^{-1}$ obtained with the harmonic mean $r_{ex} = 0.184696 \text{ \AA}$ (see Appendix A1). Thus, both angular frequencies in neutron creation and β -decay are quantized according to driving force and the resonance frequency ω_0 for each case is calculated at harmonic approximation. Note that the magnitude of the angular frequency ω_0 in the cases with $l=1$ and $l=-2$ is $\hbar\sqrt{2}$ as defined by Eq. (2).

Under meta-stable state generation, the width ($\Gamma_{1/2}$) at a half of the height in the bound state

should be proportional to the relative driving force, i.e. the ratio of antineutrino and the electron momenta, i.e. $\Gamma_{1/2} \sim p_{\bar{\nu}_e}/p_e$ and the energy gap ΔE_{pln} that arises in the hydrated neutron because of mwr -photon absorption. According to the model, antineutrino is glued with the electron under the coupling with the w -boson. Therefore, we can write the relation $p_{\bar{\nu}_e}/p_e = m_{\bar{\nu}_e} \omega_L / (m_e \omega_0)$ since the radii for the glued particles in the meta-stable state should be equal, where $\omega_L = 2\pi f_L$ ($f_L = 1057.864$ MHz) indicates the allowed level for the glued electron and neutrino particle in the excited hydrogen atom under the s - p -splitting. The charge oscillations provide the meta-stable state existence in a wide range of the angular frequencies. Neutron β -decay most likely occurs because of the attractive spin-spin interaction with the external electron under the coupling in the $\downarrow e \uparrow p \uparrow e$ moiety as depicted in Scheme 4, while the other coupled spins tend to avoid one another because of the s - p -splitting. The interactions result in neutron decay act when angular frequency of the electron reaches resonance frequency of ω_0 in the course of the charge oscillations. Then taking into account that the spin-orbit coupling (β) in the $\text{O} \cdots \text{H}^+ \cdots \text{O}$ moiety between two electrons and proton in the meta-stable state is retained before the final act and that the barrier height is $\hbar\sqrt{2}$, the width at a half of the height can be written as follows.

$$\Gamma_{1/2} = (2\sqrt{2})^{-1} \Delta E_{\text{pln}} \beta(\omega_L/\omega_0)(m_{\bar{\nu}_e}/m_e) \quad (10),$$

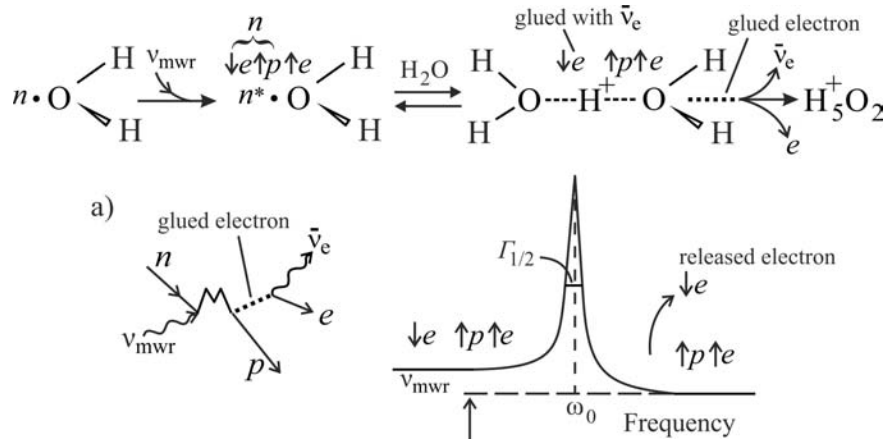
where the height $\hbar\sqrt{2}$ has been normalized on \hbar to apply Eq. (11). According to the suggested model, absorption of microwave radiation photon with the energy ν_{mwr} generates the s - p -splitting in the hydrated neutron. So then, the relation (10) for the resonance width can be rewritten taking into account Eq. (9).

$$\Gamma_{1/2} = (k_{\text{trW}} 2\sqrt{2})^{-1} \Delta E_{mwr} \beta(\omega_L/\omega_0)(m_{\bar{\nu}_e}/m_e) \quad (10a)$$

Thus, the w -boson mediates neutron β -decay as displayed in Scheme 4a, where ν_{mwr} is mwr -photon producing the s - p -splitting. As known, the width $\Gamma_{1/2}$ of a resonance produced by a meta-stable state is related to the resonance lifetime (τ) as follows.

$$\Gamma_{1/2} = \hbar/\tau \quad (11)$$

With neutrino particle mass (i.e. neutrino/antineutrino) $m_{\bar{\nu}_e} = 3.43026 \times 10^{-37}$ kg [18], $\Delta E_{\text{pln}} = 0.8723500855$ cm $^{-1}$ (or $1.732876055 \times 10^{-23}$ J), $\omega_L = 6.6465554 \times 10^9$ s $^{-1}$, and $\omega_0 = 1.5276903 \times 10^{17}$ s $^{-1}$ the calculated resonance width is $\Gamma_{1/2} = 1.195499 \times 10^{-37}$ J using Eq. (10). The same $\Gamma_{1/2} = 1.195499 \times 10^{-37}$ J is obtained with $E_{mwr} = 1.90404793$ cm $^{-1}$ ($3.7822877786 \times 10^{-23}$ J) and $k_{\text{trW}} = 2.18266492$ using Eq. (10a). Then we obtain the neutron lifetime $\tau = 882.118$ s, which is in good agreement with the lifetime of 881.5 s (deviation is 0.07%) averaged with the best seven results [4]. If we take



Scheme 4. Illustration of meta-stable state that arises after generation of the energy gap ΔE_{pln} due to mwr -photon absorption depicted in the scheme of hydrated neutron β -decay and $\hbar\sqrt{2}$ -height barrier with the resonance width ($\Gamma_{1/2}$) around ω_0 resonance frequency. Reversible arrows show transitions with H_2O displacements between the meta-stable states, one of which depicted as $\text{H}_2\text{O} \cdots \text{H}^+ \cdots \text{OH}_2$ is perturbed by proton sharing oscillations. The meta-stable state produces hydrated proton (H_3O^+), electron (e), and electronic antineutrino ($\bar{\nu}_e$) according to the diagram of the process shown in the inset a) where the driving force depicted as ν_{mwr} produces the energy gap ΔE_{pln} .

$f_L = 1045.53585$ MHz, which leads to $\omega_L = 6.5692955 \times 10^9 \text{ s}^{-1}$ and $\Delta E_{\text{pln}} = 0.8621840 \text{ cm}^{-1}$ (or $1.71268168 \times 10^{-23} \text{ J}$), then the calculated width $\Gamma_{1/2} = 1.167797 \times 10^{-37} \text{ J}$ and the lifetime $\tau = 903.043 \text{ s}$.

It should be noted that the measurement of the frequency $f = 1.4204057518 \text{ GHz}$ was published in 1963 [22], when the mean neutron lifetime was 1013 s (or half-life of the neutron was $11.7 \pm 0.3 \text{ min}$ [1]). At the same time the frequency $f_L = 1057.864 \text{ MHz}$ is a precise theoretical value of *Lamb shift* [23]. Therefore, with the latter using Eq. (4) the calculated $f_{\text{gH}} = 1.437154 \text{ GHz}$. In this case, we obtain a good agreement for the energy gap (ΔE_{nsI}) that arises because of different nucleus spin orientations in hydrogen-bonded molecules calculated by two different modes [11]. One of the modes is derived to describe the proton motion along single hydrogen bond, as depicted in Scheme 2, (see theory section) that is accompanied by the nucleus spin turnover since the absorption in the low-frequency range of Raman spectra; this mode explains the origin of boson peak in Raman and inelastic neutron scattering spectra [11, 12]. While the other takes into account hole polaron properties using Eq. (12) and the frequency $f = 1.4204057518 \text{ GHz}$ (or ΔE_{H} in cm^{-1}) [22] that gave $\Delta E_{\text{nsI}} = 40.7660 \text{ cm}^{-1}$ [11].

$$\Delta E_{\text{nsI}} = \Delta E_{\text{H}} \beta (m_{\text{p}}/m_{\text{ef}}^{\text{h}}) \beta_{\text{q}} \quad (12)$$

However, with $f_{\text{gH}} = 1.437154 \text{ GHz}$ ($\Delta E_{\text{gH}} = 0.047938297 \text{ cm}^{-1}$) using Eq. (12) the calculated $\Delta E_{\text{nsI}} = 41.247 \text{ cm}^{-1}$. The same ΔE_{nsI} is obtained by the former mode for hydrogen-bonded water molecules in gas phase [11, 12]. Thus, it seems that the frequency $f = 1.4204057518 \text{ GHz}$ measured more than fifty years ago, in fact has somewhat been changed.

Note that the resonance frequency ω_0 can be approximately obtained with the relation $\omega_0 = \alpha c/r_{\text{B}}$ too like for electron of hydrogen atom, where α and c are fine-structure constant and speed of light, respectively. However, the latter should take into consideration three-dimension walk of the electron ($\beta^{3/2}$) and $r_{\text{exI}} = 0.186666 \text{ \AA}$ (see above) instead of *Bohr radius* (r_{B}), i.e. $\omega_0 = \beta^{3/2} \alpha c/r_{\text{exI}} = 1.52332 \times 10^{17} \text{ s}^{-1}$; the deviation from $\omega_0 = 1.5276903 \times 10^{17} \text{ s}^{-1}$ is 0.3%.

3.4. Simulation of the energy spectrum of electrons from neutron β -decay according to the suggested model

It is suggested that the meta-stable state possessing antiparallel spins of the opposite charges ($\downarrow e \uparrow p \uparrow e$) as displayed in Scheme 4, which is perturbed by tetrahedral hydrogen bonding oscillations, can be decayed as follows. The antiparallel spins of the nucleus and the electron glued with antineutrino tend to avoid one another because of repulsive spin correlation effect as mentioned above. At the same time the external electron, which has the parallel (therefore, attractive) spin with the nucleus in the hydrated neutron, destroys the coupling of the opposite charges in the neutron when the resonance angular frequency ω_0 happens. The attractive spin-spin interaction, which should be proportional to the spin-orbit coupling ($\sqrt{\beta}$), involves the perturbed meta-stable state in the interaction with w -boson fluctuating state in the tetrahedron. As known, the difference between the masses of neutron and proton in the energy equivalent is $m_{\text{n}} - m_{\text{p}} = 1293.3317 \text{ keV}$. The electron glued with antineutrino in the meta-stable state should have similar maximum energy (m_{glued}^e), because the confinement energy of the electron is proportional to the spin-orbit coupling parameter depending on quaternary molecule coordination (β_{q}) under strong coupling in the tetrahedron. While under resonance conditions, golden section (R_{gold}) governs energy levels of the opposite charges [11] that should be taken into account with the factor (R_{gold}^{-1}). Therefore, the energy of the electron released at resonance angular frequency ω_0 is proportional to the coefficient ($\beta_{\text{q}} \sqrt{\beta}/R_{\text{gold}}$). Thus, the maximal energy of the glued electron is $m_{\text{glued}}^e = k_{\text{qc}} E_e = 1.28959523 \text{ MeV}$, where $E_e = m_e c^2$ and k_{qc} is the constant of four-dimension quantum well, which is defined as $k_{\text{qc}} = \beta_{\text{q}} \sqrt{\beta}/R_{\text{gold}}$ [25]. On the other hand, in hydrogen atom, where *Bohr radius* is the threshold for neutron β -decay, the relative energy of the electron is $\alpha m_e = 3.728939132 \text{ keV}$, where $\alpha = 7.297352533 \times 10^{-3}$ is thin structure constant. Then in the sum with αm_e , the maximal kinetic energy of the released electron is the value excluding the energy equivalent of the electron mass, $\Delta m_e = \alpha m_e + m_{\text{glued}}^e - m_e = 782.3253 \text{ keV}$; while w -boson fluctuations under the coupling in four-dimension quantum well lead to a decrease

of the kinetic energy of the released electron. The latter is considered as follows.

The $2p^4$ -electron orbit overlapping providing tetrahedral orientation of hydrogen bonds is diminished under H-bond bending as depicted in Scheme 2 (inset, where γ angle indicates H-bond bending) that weakens the bond strength. In general, there is no quantitative evaluation of hydrogen bonds depending on γ angle that is characterized only as ‘weak’ and ‘strong’ H-bonds. That is why this dependence has been fitted with an approximation corresponding to extent of the external electron orbit overlapping with the meta-stable state (i.e. proportionally $\cos \gamma$), spins of which are depicted as $\downarrow e \uparrow p \uparrow e$ in Scheme 4. In water tetrahedron at the moment of the neutron decay act, the released electron remains glued with antineutrino, while the spin-orbit interactions possessing different orbit overlapping at the different γ angle immediately dissipate the energy of the glued electron over the tetrahedron proportionally to the extent of the

orbit overlapping. Therefore, in the case of straight hydrogen bond, i.e. when the state with $\gamma = 0$ and $\cos(\gamma) = 1$ is realized during the molecule libration, the kinetic energy of the glued electron is dissipated over the tetrahedron proportionally to the spin-orbit coupling parameter (β_q) depending on quaternary molecule coordination, $\beta_q = 3.741657387$. So the expected most probable kinetic energy of the released (glued with antineutrino) electron should be $E_{m,k} = (\Delta m_e / \beta_q) = 209.0852$ keV. With the increase of γ angle in the course of the libration, the extent of the orbit overlapping is decreased (at first approximation) proportionally to cosine γ that leads to the less energy dissipation of the released electron. Thus, probability of the electron energy dissipation (p_γ) was assumed linear, namely $p_\gamma = \cos(\gamma)$ when $-30^\circ < \gamma < 30^\circ$, while $p_\gamma = \cos(1.07257\gamma)$ when $\gamma < -30^\circ$ and $\gamma > 30^\circ$. Thus, the kinetic energy of the released electron glued with antineutrino is retained close to Δm_e (782.3253 keV) if β -decay act happens at a large γ angle like $\gamma \sim 60^\circ$ because of the molecule libration as displayed in Fig. 3,

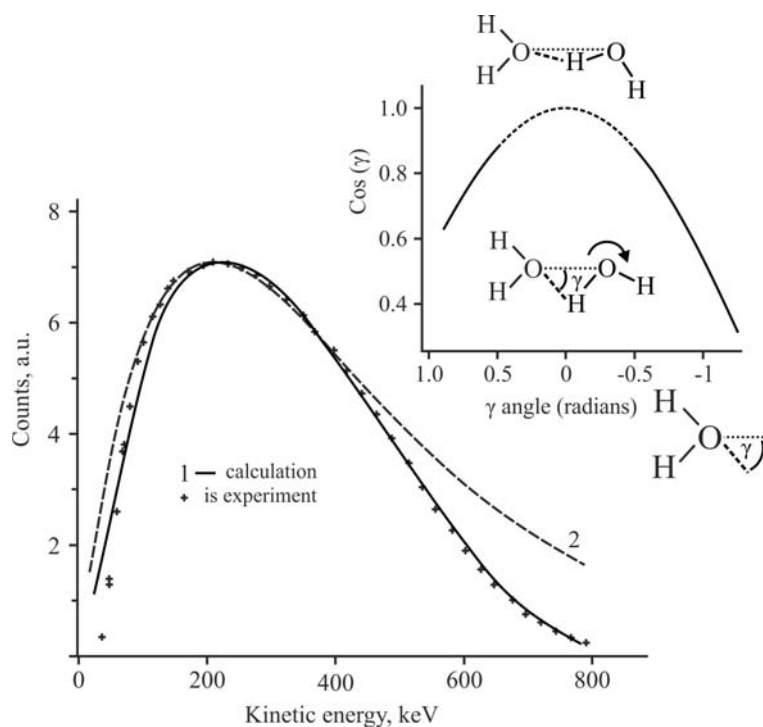


Fig. 3. Distribution of the kinetic energy of the electrons glued with antineutrino (1) under neutron β -decay as described above and calculated using Eq. (14), and the energy spectrum of electrons measured from neutron β -decay, which was reproduced using data calculated from the spectrum reported in Ref. [2]. Curve 2 was calculated using Eq. (14) in the form $P(E_k) = dN/N$, i.e. without the contribution of $p_\gamma = \cos(\gamma)$. Inset shows plot of the p_γ probability versus γ angle under the hydrogen bond bending (see details in the text).

inset. In the latter case, a small orbit overlapping prevents major energy dissipation of the released electron.

Thus, distribution of the kinetic energy of the electrons released from neutron β -decay, i.e. emitted by the perturbed meta-stable state, when the released electron is still glued with antineutrino, is proportional to the p_γ probability and the distribution, which is similar with that of *Maxwell-Boltzmann* on the velocities (v) of molecules. The corresponding relations can be written as follows, where the parameters in Eq. (14) have been replaced by the following analogues.

$$P(E_k) = p_\gamma dN/N = p_\gamma 4\pi \left\{ \frac{m}{2\pi k_B T} \right\}^{3/2} v^2 \exp(-E_k/2k_B T) dv \quad (13),$$

$$P(E_k) = p_\gamma dN/N = p_\gamma 4\pi \left\{ \frac{m_e}{2\pi E_{m,k}} \right\}^{3/2} (E_k/m_e^{1/2}) \exp(-E_k/E_{m,k}) (d\varepsilon/m_e^{1/2}) \quad (14),$$

where the electron mass is in the energy equivalent, $m_e = 510.998902$ keV, $m_e^{1/2} = m_e/2$ for electronic polaron as mentioned above, E_k and $d\varepsilon$ are the kinetic energy parameter and the energy interval, respectively. The calculated distribution of the kinetic energy is found consistent with the experimental spectrum of neutron β -decay [2] as displayed in Fig. 3.

In Fig. 3 the calculated curve 1 is somewhat different from the experiment that can be connected with the used linear dependence of p_γ probability of the electron energy dissipation under the H-bond bending. The hydrogen bonding is substantially weakened with the increase of γ angle; however, small deviations from linearity in the bond angle (such as $\gamma \sim 20^\circ$) possibly have a relatively minor effect [33]. Thus, hydrogen-bonding depending on the bond angle for water was fitted at the first approximation. It should be stressed that neutron β -decay and the backward reaction of neutron creation under antineutrino collision with proton take place in water tetrahedron, which can serve as a molecular reactor in the case of deuterium creation under x-ray radiation [18].

4. Conclusions

Thus, the suggested model for neutron β -decay describes the events of the reaction in details. This model takes into consideration that *mwr*-photon absorption by hydrated neutron or charge oscillations because of hydrogen bonding, which produces the *s-p*-splitting (ΔE_{pln}) between the $2S_{1/2}$ and $2P_{1/2}$

electron levels, generates the meta-stable state. The charge oscillations are caused by proton sharing with the frequency 3.45238 ± 0.01016 THz in water clusters estimated earlier (see above). Under *mwr*-photon absorption, similar *s-p*-splitting happens between the opposite charges glued by antineutrino, i.e. in hydrated neutron. It should be noted that neutron hydration in gas-phase water should occur like hydration of neutral atoms of argon or neon on the same reason [34, 35]. The suggested model allowed to estimate neutron lifetime that is found to be 882.118 s, which is in good agreement with the mean lifetime of 881.5 ± 1.5 s [4]. This model is based on the properties of the real *w*-boson generated between hydrogen-bonded water molecules and implies that at first antineutrino is glued with the electron as considered above for the reaction (B). The disappearance of the *s-p*-splitting with the energy gap ΔE_{pln} in polaronic exciton (or ΔE_{mwr} under hydrogen bonding with bipolaron formation) is accompanied by the emission of microwave radiation photon corresponding to blackbody radiation with the temperature 2.739497 K. The latter is consistent with $T_0 = 2.725-2.726$ K of cosmic microwave background (a deviation is 0.5%). The most probable energy of the emission obtained with $\Delta E_{mwr} = 1.9040479$ cm⁻¹ is $\nu_{mwr} = 5.38546$ cm⁻¹ (or 161.45 GHz, see Appendix A2), which is in good agreement with a maximum of the blackbody radiation at 161.0 GHz ($\nu_{mwr} = 5.37038$ cm⁻¹). Thus, according to the model, cosmic microwave background radiation originates from the reaction of neutron creation. Spectrum of the electrons from neutron β -decay simulated using *Maxwell-Boltzmann* distribution, in which parameters have been replaced by corresponding analogues, and the p_γ probability of the energy dissipation of the released electron glued with antineutrino, is found consistent with the corresponding experimental spectrum. In fact, the suggested model explains why kinetic energy of electrons, which is equivalent to the difference of $(m_n - m_p - m_e)$, emitted under neutron β -decay, is distributed in the wide energy range and the distribution has the definite shape.

Appendix A1

After antineutrino collision with proton, when the *s-p*-splitting between the $2S_{1/2}$ and $2P_{1/2}$ electron levels disappears, behavior of the polaronic exciton is defined by the system of two equations, Eqs. (2)

and (3), see above. Solving that system, we obtain relations for polaronic exciton radius r_{ex} and the angular frequency ω [19].

$$r_{\text{ex}} = [(b^2 + 4ac')^{1/2} - b]/(2a) \quad (\text{A1.1}),$$

where $a = 2\pi\omega_a m_{\text{ef}}^e = 3.2368352 \times 10^{-14} \text{ kg s}^{-1}$, $b = 2\pi(2m_{\text{ef}}^e \Delta E_k)^{1/2}$, and $c' = \hbar[l(l+1)]^{1/2}$, and

$$\omega = \hbar[l(l+1)]^{1/2}/(2\pi m_{\text{ef}}^e r_{\text{ex}}^2) \quad (\text{A1.2})$$

In the case of $l=1$, $c'=1.49138946 \times 10^{-34} \text{ J s}$ and with $\Delta E_k = 9.466476 \text{ eV}$ estimated earlier [18-19], we have $b = 7.3853940 \times 10^{-24} \text{ kg m s}^{-1}$. Then with the calculated $r_{\text{ex}1} = 0.1866663 \times 10^{-10} \text{ m}$ for this dot denoted as ω_{a1} in Fig. 2 and using Eq. (A1.2) we obtain the corresponding $\omega_{a1} = 1.495617 \times 10^{17} \text{ s}^{-1}$. The same calculation for $l = -2$ gives $r_{\text{ex}2} = 0.1788963 \times 10^{-10} \text{ m}$ with $\Delta E_k = 10.444571 \text{ eV}$ [19] and $\omega_{a2} = 1.628356 \times 10^{17} \text{ s}^{-1}$. Then with harmonic mean $r_{\text{ex}} = 0.184696 \text{ \AA}$ (see section 3.3), which is obtained for neutron β -decay, the calculated resonance frequency is $\omega_0 = 1.5276903 \times 10^{17} \text{ s}^{-1}$.

Appendix A2

The spectrum of blackbody radiation was calculated using *Planck law* [36] expressed *via* the frequency (f) that is shown in Fig. 4.

$$\varepsilon(f, T) = 2\pi h f^3 / c^2 \{ 1 / [\exp(hf/k_B T) - 1] \} \quad (\text{A2.1}),$$

where h and k_B are *Planck* and *Boltzmann* constants, respectively and c is the speed of light.

Under neutron creation, when resonance angular frequency ω_0 happens, the electron should overcome the $\hbar\sqrt{2}$ height barrier twice during the molecule libration, i.e. in the course of 2π turns (see Fig. 2). Therefore, the most probable energy of the *mwr*-photon emitted under neutron creation, when the energy gap ΔE_{mwr} disappears, should be proportional to $2\sqrt{2}$, namely $\nu_{\text{mwr}} = 2\sqrt{2} \times \Delta E_{\text{mwr}} = 2\sqrt{2} \times 1.8952263 \text{ cm}^{-1} = 5.3605 \text{ cm}^{-1}$ (160.70 GHz). The same spectrum of the microwave radiation but with a maximum at 161.0 GHz has been obtained using Eq. (A2.1) with the above temperature of 2.739497 K. In the latter case, the most probable energy of the microwave emission is $\nu_{\text{mwr}} = 5.38546 \text{ cm}^{-1}$ (or 161.45 GHz) that is obtained with $\Delta E_{\text{mwr}} = 1.9040479 \text{ cm}^{-1}$. Both calculated spectra of the blackbody radiation obey the cosmic microwave background spectrum reproduced using the full *COBE FIRAS Data Set* [26].

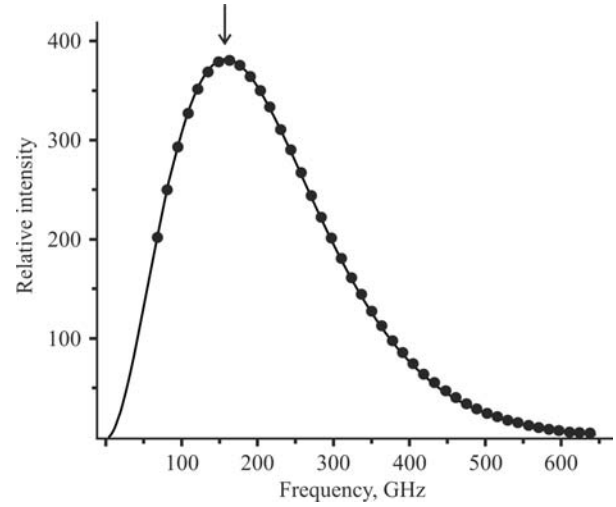


Fig. 4. Plot of blackbody radiation using Eq. (A2.1) with $T = 2.726805 \text{ K}$ under neutron creation accompanied by disappearance of the energy gap ΔE_{mwr} ; the arrow indicates a maximum at the frequency of 158.61 GHz. Filled circles show the spectrum of cosmic microwave background radiation plotted using *COBE FIRAS Data* [26].

Appendix A3

The difference (ΔE_L) between the $2S_{1/2}$ and $2P_{1/2}$ electron levels that arises as *Lamb shift* in the hydrogen excited state directly implies the spin-orbit coupling ($\sqrt{\beta}$) of the electron with proton in polaronic exciton; therefore, the electron behavior depends on the proton delocalization within the tetrahedron. Then with the use of *Lamb shift* (ΔE_L) for atomic hydrogen, *s-p*-splitting (ΔE_{pln}) between the $2S_{1/2}$ and $2P_{1/2}$ electron levels in polaronic exciton composed by proton and its own electron should be written taking into account the spin-orbit coupling ($\sqrt{\beta}$) for three-dimension walk of the electron coupled with the proton and the ratio of the effective masses.

$$\Delta E_{\text{pln}} = \Delta E_L \beta^{3/2} (m_{\text{ef}}^h / m_{\text{ef}}^e) \quad (\text{A3.1})$$

For the hydrogen-bonded water molecules, where golden section (R_{gold}) governs the levels of the coupled electron and proton establishing the hydrogen bond [11], the *s-p*-splitting between the $2S_{1/2}$ and $2P_{1/2}$ electron levels (ΔE_{sp}) should be additionally proportional to the golden section because of the proton sharing as depicted in Scheme 2.

$$\Delta E_{\text{sp}} = R_{\text{gold}} \Delta E_{\text{pln}} = \Delta E_L \beta^{3/2} R_{\text{gold}} (m_{\text{ef}}^h / m_{\text{ef}}^e) \quad (\text{A3.2})$$

With $\Delta E_L = 0.0352865448 \text{ cm}^{-1}$ ($f_L = 1057.864$

MHz [23]), $\beta = 1.19100654$, $m_{\text{ef}}^{\text{h}} = 9.51m_{\text{e}}$, and $m_{\text{ef}}^{\text{c}} = 0.5m_{\text{e}}$ the calculated $\Delta E_{\text{pln}} = 0.8723500855 \text{ cm}^{-1}$ and $\Delta E_{\text{sp}} = 1.41149 \text{ cm}^{-1}$, the latter is almost the same as 1.41153 cm^{-1} on average estimated with Eq. (A3.2) earlier [12]. Theoretical s - p -splitting (ΔE_{sp}) between the $2S_{1/2}$ and $2P_{1/2}$ electron levels obtained earlier is supported by an experimental energy gap of 1.4176 cm^{-1} [25].

Conflict of interest statement

The author declares no conflict of interests.

References

1. Miles, R. F. (Jr.), 1963, The Density of Cosmic-Ray Neutrons in the Atmosphere, PhD. Thesis, California Institute of Technology, Pasadena.
2. Basdevant, J.-L., Rich, J. and Spiro, M. 2005, Fundamentals in Nuclear Physics, Springer Science & Business Media, Inc., New York.
3. Yao, W.-M., Amsler, C., Asner, D., Barnett, R. M., Beringer J., Burchat, P. R., Carone C. D., Caso, C., Dahl O., D'Ambrosio, G., De Gouvea, A., Doser, M., Eidelman, S., Feng, J. L., Gherghetta, T., Goodman, M., Grab, C., Groom, D. E., Gurtu, A., Hagiwara, K., Hayes, K. G., Hernández-Rey, J. J., Hikasa, K., Jawahery, H., Kolda, C., Kwon, Y., Mangano M. L., Manohar, A. V., Masoni, A., Miquel, R., Mönig, K., Murayama, H., Nakamura, K., Navas, S., Olive, K. A., Pape, L., Patrignani, C., Piepke, A., Punzi, G., Raffelt, G., Smith, J. G., Tanabashi, M., Terning, J., Törnqvist, N. A., Trippe, T. G., Vogel, P., Watari, T., Wohl, C. G., Workman, R. L. and Zyla, P. A. (Particle Data Group), 2006, J. Phys. G, 33, 1, <http://pdg.lbl.gov>
4. Beringer, J., Arguin, J.-F., Barnett, R. M., Copic, K., Dahl, O., Groom, D. E., Lin, C.-J., Lys, J., Murayama, H., Wohl, C. G., Yao, W.-M., Zyla, P. A., Amsler, C., Antonelli, M., Asner, D. M., Baer, H., Band, H. R., Basaglia, T., Bauer, C. W., Beatty, J. J., Belousov, V. I., Bergren, E., Bernardi, G., Bertl, W., Bethke, S., Bichsel, H., Biebel, O., Blucher, E., Blusk, S., Brooijmans, G., Buchmueller, O., Cahn, R. N., Carena, M., Ceccucci, A., Chakraborty, D., Chen, M.-C., Chivukula, R. S., Cowan, G., D'Ambrosio, G., Damour, T., de Florian, D., de Gouvêa, A., De Grand, T., de Jong, P., Dissertori, G., Dobrescu, B., Doser, M., Drees, M., Edwards, D. A., Eidelman, S., Erler, J., Ezhela, V. V., Fetscher, W., Fields, B. D., Foster, B., Gaisser, T. K., Garren, L., Gerber, H.-J., Gerbier, G., Gherghetta, T., Golwala, S., Goodman, M., Grab, C., Gritsan, A. V., Grivaz, J.-F., Grünewald, M., Gurtu, A., Gutsche, T., Haber, H.E., Hagiwara, K., Hagmann, C., Hanhart, C., Hashimoto, S., Hayes, K. G., Heffner, M., Heltsley, B., Hernández-Rey, J. J., Hikasa, K., Höcker, A., Holder, J., Holtkamp, A., Huston, J., Jackson, J. D., Johnson, K. F., Junk, T., Karlen, D., Kirkby, D., Klein, S. R., Klempt, E., Kowalewski, R. V., Krauss, F., Kreps, M., Krusche, B., Kuyanov, Yu. V., Kwon, Y., Lahav, O., Laiho, J., Langacker, P., Liddle, A., Ligeti, Z., Liss, T. M., Littenberg, L., Lugovsky, K. S., Lugovsky, S. B., Mannel, T., Manohar, A. V., Marciano, W. J., Martin, A. D., Masoni, A., Matthews, J., Milstead, D., Miquel, R., Mönig, K., Moortgat, F., Nakamura, K., Narain, M., Nason, P., Navas, S., Neubert, M., Nevski, P., Nir, Y., Olive, K. A., Pape, L., Parsons, J., Patrignani, C., Peacock, J. A., Petcov, S. T., Piepke, A., Pomarol, A., Punzi, G., Quadt, A., Raby, S., Raffelt, G., Ratcliff, B. N., Richardson, P., Roesler, S., Rolli, S., Romaniouk, A., Rosenberg, L. J., Rosner, J. L., Sachrajda, C. T., Sakai, Y., Salam, G. P., Sarkar, S., Sauli, F., Schneider, O., Scholberg, K., Scott, D., Seligman, W. G., Shaevitz, M. H., Sharpe, S. R., Silari, M., Sjöstrand, T., Skands, P., Smith, J. G., Smoot, G. F., Spanier, S., Spieler, H., Stahl, A., Stanev, T., Stone, S. L., Sumiyoshi, T., Syphers, M. J., Takahashi, F., Tanabashi, M., Terning, J., Titov, M., Tkachenko, N. P., Törnqvist, N. A., Tovey, D., Valencia, G., van Bibber, K., Venanzoni, G., Vinciter, M. G., Vogel, P., Vogt, A., Walkowiak, W., Walter, C. W., Ward, D. R., Watari, T., Weiglein, G., Weinberg, E. J., Wiencke, L. R., Wolfenstein, L., Womersley, J., Woody, C. L., Workman, R. L., Yamamoto, A., Zeller, G. P., Zenin, O. V., Zhang, J. and Zhu, R.-Y. (Particle Data Group), 2012, Phys. Rev., D86, 1, <https://doi.org/10.1103/PhysRevD.86.010001>

5. Serebrov, A., Varlamov, V., Kharitonov, A., Fomin, A., Pokotilovski, Yu., Geltenbort, P., Butterworth, J., Krasnoschekova, I., Lasakov, M., Tal'daev, R., Vassiljev, A. and Zherebtsov, O. 2005, *Phys. Lett. B*, 605, 72.
6. Feynman, R. P., Leighton, R. B. and Sands, M. 1966, *The Feynman Lectures on Physics*, Mir, Moscow, V. 6 (Russian).
7. Kumar, P., Wikfeldt, K. T., Schlesinger, D., Pettersson, L. G. M. and Stanley, H. E. 2013, *Sci. Rep.*, 3, 1980.
8. Wang, Z., Liu, K.-H., Le, P., Li, M., Chiang, W.-S., Leao, J. B., Copley, J. R. D., Tyagi, M., Podlesnyak, A., Kolesnikov, A. I., Mou, C.-Y. and Chen, S.-H. 2014, *Phys. Rev. Lett.*, 112, 237802.
9. Schroeder, J., Wu, W., Apkarian, J. L., Lee, M., Hwa, L.-G. and Moynihan, C. T. 2004, *J. Non-Cryst. Solid.*, 349, 88.
10. Kabeya, M., Mori, T., Fujii, Y., Koreeda, A., Wan Lee, B., Ko, J.-H. and Kojima, S. 2016, *Phys. Rev. B*, 94, 224204.
11. Udaltsov, A. V. 2018, *Vibr. Spectrosc.* 97, 16. Corrigendum to *Vibr. Spectrosc.* 2018, 97, 16: *Vibr. Spectrosc.* 2018, 99, 204.
12. Udaltsov, A. V. 2018, *Chem. Phys.*, 511, 46.
13. Atkins, P. and Friedman, R. 2005, *Molecular Quantum Mechanics*, Oxford, New York, Oxford University Press, 4th ed.
14. Udaltsov, A. V. 2018, *J. Mol. Spectrosc.*, 345, 22.
15. Udaltsov, A. V. 2017, *J. Mol. Liquid.*, 227, 262.
16. Udaltsov, A. V. 2015, *J. Phys. Chem., Sol.*, 86, 162.
17. Udaltsov, A. V. 2016, *J. Mol. Struct.*, 1125, 522.
18. Udaltsov, A. V. 2017, *J. Mol. Liquid.*, 237, 99.
19. Udaltsov, A. V. 2017, *J. Ener. Power Eng.*, 11, 693, doi:10.17265/1934-8975/2017.11.003
20. Page L. and Wilkinson D. 1999, *Rev. Modern Phys.*, 71, 173.
21. Smoot, G. F. 2007, *Rev. Mod. Phys.*, 79, 1349.
22. Feynman, R. P., Leighton, R. B. and Sands, M. 1966, *The Feynman Lectures on Physics*, Mir, Moscow, V. 8 (Russian).
23. Das, A. and Sidharth, B. G. 2015, *Electron. J. Theor. Phys.*, 12, 139.
24. Itzykson, C. and Zuber, J. B. 1984, *Quantum Field Theory*, Moscow, Mir, Vol. 1. (Russian).
25. Udaltsov, A. V. 2019, *J. Mol. Liquid.*, 293, <https://doi.org/10.1016/j.molliq.2019.111499>
26. Fixsen, D. J., Cheng, E. S., Gales, J. M., Mather, J. C., Shafer, R. A. and Wright, E. L. 1996, *Astrophys. J.*, 473, 576.
27. Rufflé, B., Parshin, D. A., Courtens, E. and Vacher, R. 2008, *Phys. Rev. Lett.*, 100, 15501.
28. Mallamace, F., Corsaro, C., Mallamace, D., Wang, Z. and Chen, S.-H. 2015, *Front. Phys.*, 10, 106103.
29. Udaltsov, A. V. 2018, *Proceedings 2*, 1112, <http://www.mdpi.com/2504-3900/2/14/1112>
30. Nilsson, A. and Pettersson, L. G. M. 2011, *Chem. Phys.*, 389, 1.
31. Chaplin, M. F. *Water Absorption Spectrum*, updated by M. Chaplin on 1 July, 2017 (accessed), http://www1.lsbu.ac.uk/water/water_vibrational_spectrum.html
32. Guo, J.-H., Luo, Y., Augustsson, A., Rubensson, J.-E., Sâthe, C., Ågren, H., Siegbahn, H. and Nordgren, J. 2002, *Phys. Rev. Lett.*, 89, 137402.
33. Rao, C. N. R. 1972, *Theory of Hydrogen Bonding in Water*, in: *The Physics and Physical Chemistry of Water*, F. Franks (Ed.), Plenum Press, New York, 93.
34. Headrick, J. M., Diken, E. G., Walters, R. S., Hammer, N. I., Christie, R. A., Cui, J., Myshakin, E. M., Duncan, M. A., Johnson, M. A. and Jordan, K. D. 2005, *Science*, 308, 1765.
35. Headrick, J. M., Bopp, J. C. and Johnson, M. A. 2004, *J. Chem. Phys.*, 121, 11523.
36. Fermi, E. 1947, *Molecules and Crystals*, Inostr. Lit. Publ., Moscow (Russian). Transl. from German language: Fermi, E. 1938, *Moleküle und Kristalle*, Barth J.A. Publ., Leipzig.